

Signatures of quantum chaos in complex wavefunctions describing open billiards

This article has been downloaded from IOPscience. Please scroll down to see the full text article.

2005 J. Phys. A: Math. Gen. 38 10787

(<http://iopscience.iop.org/0305-4470/38/49/019>)

View [the table of contents for this issue](#), or go to the [journal homepage](#) for more

Download details:

IP Address: 171.66.16.94

The article was downloaded on 03/06/2010 at 04:04

Please note that [terms and conditions apply](#).

Signatures of quantum chaos in complex wavefunctions describing open billiards

Almas F Sadreev^{1,2} and Karl-Fredrik Berggren²

¹ Kirensky Institute of Physics, 660036 Krasnoyarsk, Russia

² Department of Physics and Measurement Technology, Linköping University, SE-581 83 Linköping, Sweden

E-mail: almasa@ifm.liu.se, almas@tnp.krasn.ru and kfber@ifm.liu.se

Received 25 May 2005, in final form 3 August 2005

Published 22 November 2005

Online at stacks.iop.org/JPhysA/38/10787

Abstract

We discuss signatures of quantum chaos in open chaotic billiards. Solutions for such a system are given by complex scattering wavefunctions $\psi = u + iv$ when a steady current flows through the billiard. For slightly opened chaotic billiards the current distributions are simple and universal. It is remarkable that the resonant transmission through integrable billiards also gives the universal current distribution. Currents induced by the Rashba spin–orbit interaction can flow even in closed billiards. Wavefunction and current distributions for a chaotic billiard with weak and strong spin–orbit interactions have been derived and compared with numerics. Similarities with classical waves are considered. In particular we propose that the networks of electric resonance RLC circuits may be used to study wave chaos. However, being different from quantum billiards, there is a resistance from the inductors which gives rise to heat power and decoherence.

PACS number: 05.45.Mt

1. Introduction

1.1. Closed billiards

The nature of quantum chaos in a specific system is traditionally inferred from its classical counterpart. It is an interdisciplinary field that extends into, for example, atomic and molecular physics, condensed matter physics, nuclear physics and subatomic physics [1]. The main achievement of this field is the establishment of universal statistics of energy levels in chaotic versus integrable quantum systems. The latter were shown to be faithful to Poisson statistics of independent energy levels, whereas the former turned out to be well described by theory of large Gaussian random matrices (RMT) introduced by Wigner [2] to explain statistical

fluctuations of neutron resonances in a compound nucleus. Rather than trying to explain individual eigenvalues, RMT addresses questions about their statistical behaviour. Its original justification was our lack of knowledge of the exact Hamiltonian; RMT assumes maximal ignorance regarding the system's Hamiltonian except that it must be consistent with the underlying symmetries. The theory proceeds to construct ensembles of Hamiltonians classified by their symmetry. Wigner's ideas were followed by those of Porter and Rosenzweig [3] and Mehta and Gaudin [4, 5]. Dyson [6] showed that there are three classes of random-matrix ensembles (GOE, GUE and GSE).

Two major independent developments in the early 1980s considerably broadened the range of validity of RMT. One was the BGS conjecture (Bohigas, Giannoni and Schmit [7]) linking the quantal fluctuations in chaotic systems to RMT. The second major development was Efetov's supersymmetry method [8], which made possible a nonperturbative treatment of the single-particle disorder problem by mapping it onto the supersymmetric nonlinear σ model. The random-matrix theory has many applications in quantum physics; a comprehensive review emphasizing common concepts was written recently by Guhr *et al* [9].

Today one finds an increase in experimental studies [10]. For example, one can now fabricate well-defined ultra-small chaotic systems from semiconductor materials by means of nanotechnology. As we will describe here, that quantum chaos is closely related to classical wave chaos as found for irregular microwave and acoustic cavities. Recently experimental studies of chaotical optical billiards for ultracold atoms [12, 13] and for the Bose–Einstein condensate [14] have begun.

Next, consider statistical properties of the eigenfunctions of the chaotic two-dimensional quantum billiards in the hard wall approximation

$$-\nabla^2 \psi_n(x, y) = \epsilon_n \psi_n(x, y), \quad (1)$$

where the Dirichlet boundary condition is implied at the boundary Ω of the billiard: $\psi|_{\Omega} = 0$. Here we use Cartesian coordinates x, y which are dimensionless via a characteristic size of the billiard L , and correspondingly $\epsilon_n = k_n^2 = E_n/E_0$, $E_0 = \hbar^2/2mL^2$. Shapiro and Goelman [15] first presented statistics of the eigenfunctions although their numerical histogram $P(\psi)$ was not compared with the Gaussian distribution. This was done by McDonnell and Kauffmann [16] who concluded that the majority ($\approx 90\%$) of the eigenfunctions of the Bunimovich billiard are a Gaussian random field (RGF) for all x, y . Also McDonnell and Kauffmann revealed characteristic complex patterns of disordered, curvilinear and non-crossing nodal lines. Such features have also been observed experimentally for microwave cavities [1, 17] and acoustic resonators [18].

These results nicely agree with the Berry conjecture [19] of quantum chaos according to which the wavefunction in the chaotic billiard has to be expressed as a sum over an infinite number of plane waves

$$\psi(x, y) = \sum_j a_j \exp[i(\mathbf{k}_j \mathbf{r} + \phi_j)] \quad (2)$$

each having a random amplitude a_j , phase ϕ_j and direction \mathbf{k}_j but equal length $|k_j|^2 = \epsilon$. In closed chaotic billiards, we are to take the real part of (2). This leads to a Gaussian amplitude distribution and a spatial correlation function with Bessel function dependence. This conjecture, in fact, was raised by Rayleigh [20].

However, there exist also eigenfunctions which behave otherwise. Most of them are localized on families of regular classical trajectories (scars [21]) or bouncing ball modes [16]). Their number behaves as $N_{bb}(E) = \alpha E^\delta$ with $\alpha = 0.2$, $\delta = 3/4$ [22, 23].

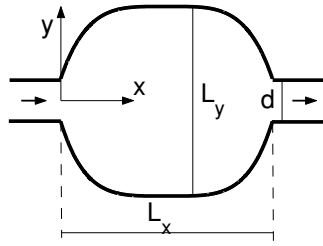


Figure 1. Schematic geometry of transmission through a billiard.

1.2. Open billiards

The typical way to open a billiard is to attach some reservoirs with continuous energy spectrum, for example, the leads or microwave waveguides, as shown in figure 1. Most experiments on wave transmission are performed for this geometry. Another way to open the billiard is to include processes of inelastic scattering, i.e. to take absorption into account. This means that the billiard is also connected to a reservoir but not locally as shown in figure 1.

Full information about the scattering properties of the billiard is given by the scattering wavefunction which is a solution of the Schrödinger equation $H\psi = E\psi$ with the total Hamiltonian

$$H = H_B + H_L + H_R + V, \quad (3)$$

where H_B is the Hamiltonian of the closed quantum system, in the present case the billiard with a spectrum given by equation (1), $H_L + H_R$ describes two leads (the left and right ones as shown in figure 1) with continuous spectrum and $V = V_L + V_R$ is the coupling between the closed system and the leads. The mathematical tool to treat scattering processes is provided by scattering theory [24–28] which has been successfully applied to billiards [1, 29–33]. Assume, we know the coupling matrices W_C , $C = L, R$ of rank $M \times N$ where M is the number of channels in the leads and N is the number of bound states of closed billiard. The finite number N is artificial and can eventually be taken to infinity. Then statistical properties of transmission through a billiard can be related to those of the resolvent of effective non-Hermitian Hamiltonian

$$H_{\text{eff}} = H_B - i\pi \sum_{C=L,R} W_C^+ W_C. \quad (4)$$

The complex eigenvalues of the effective Hamiltonian determine positions and widths of the resonances. To the best of our knowledge, the concept of the effective Hamiltonian appeared first in Feshbach's papers [24] and, independently, in Livshits's study of open quantum system [34].

The idea was to adjust RMT to a description of open quantum chaotic billiards starting from the effective Hamiltonian and following the same lines as for their closed counterparts goes back to the pioneering work [35]; see also [30, 36] and references therein. The starting point of this approach is the representation of the scattering matrix S in terms of an effective non-Hermitian Hamiltonian $H_{\text{eff}} = H_B - i\Gamma$, where the anti-Hermitian part $i\Gamma$ arises due to coupling to open scattering channels as seen from (4). It has to be chosen in the form ensuring the unitarity of the scattering matrix. A natural way to incorporate the random-matrix description of the quantum chaotic system is to replace H_B by a large $N \times N$ random-matrix of appropriate symmetry. Namely, chaotic systems with preserved time-reversal invariance (TRI) should be described by matrices H_B which are real symmetric. Such matrices form

the GOE, whereas for systems with broken TRI one uses complex Hermitian matrices from the GUE. In general, the two matrices H_B and Γ do not commute, making the analysis of complex eigenvalues of H_{eff} to be a rather non-trivial problem [36, 37]. Another way is an application to closed billiard of magnetic field that breaks the TRI [30, 38]. For intermediate magnetic fields, a crossover occurs between the GOE and the GUE where the parameter

$$\epsilon^2 = \frac{\langle \text{Im}(\psi)^2 \rangle}{\langle \text{Re}(\psi)^2 \rangle} \quad (5)$$

governs this crossover. The parameter ϵ in (5) is closely related to the phase rigidity of the wavefunction, first introduced by van Langen *et al* [39]

$$r = \frac{\langle \psi^2 \rangle}{\langle |\psi|^2 \rangle}. \quad (6)$$

The relation between these two parameters is simple

$$r = \left(\frac{1 - \epsilon^2}{1 + \epsilon^2} \right). \quad (7)$$

Quantum mechanically, the ‘openness’ may be related to decays into open channels [31, 40–42]. It can be enlarged either by increasing the number of open channels or by enhancing the (average) coupling strength between bound states and a given decay channel [31]. Definition of the effective Hamiltonian (4) gives a measure of openness of the billiard as $\gamma = \Gamma/E$, where $\Gamma = \frac{1}{N} \sum_{\lambda} \text{Im}(z_{\lambda})$ is the mean width, z_{λ} are the complex eigenvalues of H_{eff} , and E is the energy. The imaginary part of H_{eff} is given by the coupling matrix. A recipe how to calculate the matrix elements W_C is given in [31–33, 43]. For the coupling with the left lead in the Cartesian coordinates shown in figure 1, we write

$$W = \sqrt{\frac{1}{\pi k}} \int_0^d dy \phi_m(y) \frac{\partial}{\partial x} \psi_B \quad (x = 0, y), \quad (8)$$

where $\phi_m(y) = \sqrt{\frac{1}{2d}} \sin\left(\frac{\pi m y}{d}\right)$, $m = 1, 2, 3, \dots$ are the eigenfunctions of the lead, $\psi_B(x, y)$ are the eigenfunctions of the billiard normalized by equation $\int_A dx dy \psi_B(x, y)^2 = 1$. For the right lead $x = L_x$. Evaluating $\frac{\partial}{\partial x} \psi_B(x = 0, y)$ as $k \psi_B(x = 0, y)$, where k is the wave number of incidenting particle and substituting these definitions into (8) one obtains first estimate of the coupling $W \sim \sqrt{kd/A}$. Taking the eigenvalues of the billiard resonant to the energy of incidenting particle k^2 we obtain that the measure of openness of the billiard is given by the ratio

$$\gamma = \frac{Md}{Ak}. \quad (9)$$

One finds from (9) that the openness is defined by the number of channels M and aspect ratio d/A , i.e. ratio of the cross-section of lead to the area of the closed billiard. Results of numerical calculation of the complex eigenvalues of (4) for the transmission through rectangular billiard with use of lattice theory of the scattering matrix [33] are shown in figure 2. Figure clearly shows the way Γ grows with opening of channels at points $E = \pi^2 m^2$ marked by open circles, as well as its growth with increasing the aspect ratio d^2/A .

2. The wavefunction and current statistics

If there is a stationary current via the leads as shown in figure 1 we have the scattering wavefunction which violates the TRI. Even if the Hamiltonian itself is invariant under the TRI, the statistics of the scattering wavefunction will not follow the GOE [45–47].

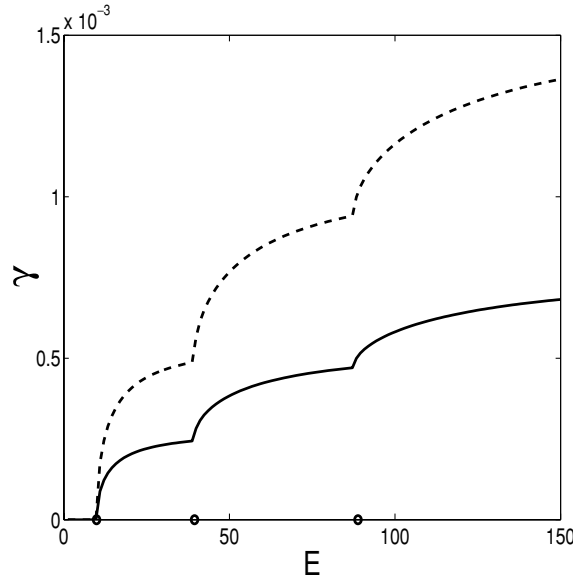


Figure 2. Dependence of the parameter of openness (9) on the energy E in terms of $\hbar^2/2md^2$ for the transmission through rectangular billiard. The aspect ratio $d^2/A = 0.1$ (solid line) and $d^2/A = 0.2$ (dashed line).

The scattering wavefunction $H\psi = E\psi$ can be mapped onto the interior space of the billiard by the projection operator $\psi_B = P_B\psi$ where $P_B = \sum_n |n\rangle\langle n|$. Then this truncated scattering wavefunction can be expanded in the eigenfunctions of the closed billiard $\psi_n(x, y)$ [33]. For a single-channel transmission one has

$$\psi_B(\mathbf{r}) = \sum_{nn'} \sum_{C=L,R} W_C(n')\langle n'| \frac{1}{E + i0 - H_{\text{eff}}} |n\rangle \psi_n(\mathbf{r}) = \sum_n c_n \psi_n(\mathbf{r}). \quad (10)$$

If the contribution of the localized eigenfunctions (scars or bouncing ball modes) in (10) is negligible, then all eigenfunctions $\psi_n(\mathbf{r})$ are RGF. The complex coefficients in the superposition, c_n , depend on the energy and the coupling between the billiard and leads and are not random as in the Berry function (2). Nonetheless the superposition of RGFs is also a complex RGF [48, 49]

$$\psi_B(\mathbf{r}) = u(\mathbf{r}) + iv(\mathbf{r}). \quad (11)$$

Even for the resonant transmission through the Sinai billiard, computations show that many eigenfunctions contribute to the scattering wavefunction as shown in figure 3. More obvious presentation for the scattering wavefunction was used by Pnini and Shapiro [45] in the form of the Berry-like function

$$\psi_B(\mathbf{r}) = \sum_n \{\cos(\theta_n + \mathbf{k}_n \mathbf{r}) + \lambda \exp[i(\phi_n + \mathbf{k}_n \mathbf{r})]\}, \quad (12)$$

where the random standing waves are responsible for closed chaotic billiard whereas the random travelling waves describe coupling of the billiard to the external world via the parameter λ .

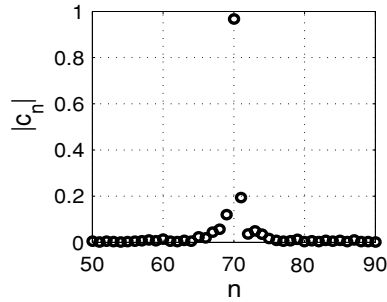


Figure 3. The coefficients $|c_n|$ in expansion (10) for the resonant transmission through the Sinai billiard with numerical sizes 500×500 , $R = 50$ with energy $E = 10.425$.

An assumption of a complex RGF for the scattering function (11) means that the joint probability density has the form

$$f(u, v) = \frac{1}{2\pi\sqrt{\langle u^2 \rangle \langle v^2 \rangle - \langle uv \rangle}} \exp\left(-\frac{u^2}{2\langle u^2 \rangle} - \frac{v^2}{2\langle v^2 \rangle} + \frac{uv}{2\langle uv \rangle}\right). \quad (13)$$

First of all, following [50] we perform a phase transformation

$$\psi(\mathbf{x}) \rightarrow e^{i\alpha} \psi(\mathbf{x}) = p(\mathbf{x}) + iq(\mathbf{x}) \quad (14)$$

to new functions $p(\mathbf{x})$ and $q(\mathbf{x})$ with condition that the statistical average $\langle pq \rangle = 0$. This step eliminates phase ambiguity and ensures that RGFs p and q are statistically independent. This phase transformation (14) corresponds to diagonalization of the quadratic form in (13) [51]:

$$f(p, q) = f(p)f(q), \quad f(x) = \frac{1}{\sqrt{2\pi\langle x^2 \rangle}} \exp\left(-\frac{x^2}{2\langle x^2 \rangle}\right). \quad (15)$$

This step is a matter of convenience which simplifies calculations. For example, calculation of the distribution of intensity $\rho = |\psi_B|^2$ becomes elementary and gives the following probability density distribution $\rho = |\psi|^2$,

$$f(\rho) = \mu \exp(-\mu^2 \rho) I_0(\mu v \rho), \quad (16)$$

with the following notations

$$\mu = \frac{1}{2} \left(\frac{1}{\epsilon} + \epsilon \right), \quad v = \frac{1}{2} \left(\frac{1}{\epsilon} - \epsilon \right), \quad (17)$$

and $I_0(x)$ is the modified Bessel function of zeroth order. Formula (16) was obtained by many approaches [38, 45–47, 52].

The distribution (16) depends parametrically on ϵ (5) or r (6). In fact, these parameters strongly fluctuate with variation of energy E [44, 51] that leads to different results for averages taken over $\mathbf{r} = (x, y)$ only as compared to one over both r and E [44]. Therefore, an average over E implies an additional average over ϵ or r . The distribution $P(r)$ was first calculated by Sommers and Iida [53]. Brouwer has shown that fluctuations of phase rigidity (6) cause long-range correlations of intensity ρ and current density [44]. These correlations were measured by Kim *et al* [54] with perfect agreement with theoretical results [44].

As for the next tutorial of a RGF we consider current distributions. The expression for current,

$$\mathbf{j} = p\nabla q - q\nabla p, \quad (18)$$

shows that the distribution for one component of the current density, say j_x we need the Gaussian probability density $f(p, p_x, q, q_x)$ [55]. The density and its corresponding characteristic functions are completely determined by the covariance matrix of the field variables

$$\mathbf{M} = \begin{pmatrix} \langle p^2 \rangle & \langle pq_x \rangle & \langle pq \rangle & \langle pp_x \rangle \\ \langle pq_x \rangle & \langle q_x^2 \rangle & \langle qq_x \rangle & \langle p_x q_x \rangle \\ \langle pq \rangle & \langle qq_x \rangle & \langle q^2 \rangle & \langle qp_x \rangle \\ \langle pp_x \rangle & \langle p_x q_x \rangle & \langle qp_x \rangle & \langle p_x^2 \rangle \end{pmatrix} = \begin{pmatrix} \langle p^2 \rangle & \langle pq_x \rangle & 0 & 0 \\ \langle pq_x \rangle & \langle q_x^2 \rangle & 0 & 0 \\ 0 & 0 & \langle q^2 \rangle & \langle qp_x \rangle \\ 0 & 0 & \langle qp_x \rangle & \langle p_x^2 \rangle \end{pmatrix}. \quad (19)$$

The covariance matrix may be simplified further if we assume that we deal with isotropic fields for which ∇p and ∇q are statistically independent of p and q [50]. The Berry function (2) is typical example of isotropic RGF. Then $\langle p \nabla q \rangle = \langle q \nabla p \rangle = 0$ and as follows from (18), the net current $\langle \mathbf{j} \rangle = 0$. As shown in [51] that is the case if the transmission is near zero. Correspondingly the Gaussian probability density factorizes as

$$f(p, p_x, q, q_x) = f(p)f(q)f(p_x)f(q_x), \quad (20)$$

where

$$f(p_x) = \frac{1}{\sqrt{2\pi\langle p_x^2 \rangle}} \exp\left(-\frac{p_x^2}{2\langle p_x^2 \rangle}\right), \quad f(q_x) = \frac{1}{\sqrt{2\pi\langle q_x^2 \rangle}} \exp\left(-\frac{q_x^2}{2\langle q_x^2 \rangle}\right). \quad (21)$$

In particular this is the case for the Berry function (2) with $\langle p^2 \rangle = \langle q^2 \rangle$, $\langle p_x^2 \rangle = \langle q_x^2 \rangle$.

Now it is easy to calculate the current distribution functions. For the x component we have

$$P(j_x) = \langle \delta(j_x - pq_x + qp_x) \rangle = \frac{1}{2\pi} \int_{-\infty}^{\infty} \Theta(a_x) e^{-ia_x j_x} da_x, \quad (22)$$

where

$$\Theta(a_x) = \int dp dq dp_x dq_x f(p)f(q)f(p_x)f(q_x) e^{ia_x(pq_x - qp_x)} = \frac{1}{1 + a_x^2 \tau^2}, \quad (23)$$

$$\tau^2 = \langle p^2 \rangle \langle q_x^2 \rangle = \langle q^2 \rangle \langle p_x^2 \rangle = \frac{1}{2} k^2 \langle p^2 \rangle \langle q^2 \rangle = \frac{k^2 \epsilon^2}{2(1 + \epsilon^2)} \quad (24)$$

provided that $\langle p^2 \rangle + \langle q^2 \rangle = 1$ (normalization condition), and ϵ is the parameter of openness of the billiard (5). Finally substituting equations (23) and (24) into (22) we obtain the very simple form of the distribution of the x component of current

$$P(j_x) = \frac{1}{2\tau} \exp\left(-\frac{|j_x|}{\tau}\right). \quad (25)$$

For the case nonzero net current the distribution takes the following form [55]:

$$P(j_x) = \frac{1}{2\tau} \exp\left\{-\frac{|j_x|}{\tau} + \frac{\langle j_x \rangle j_x}{2\tau^2}\right\}. \quad (26)$$

The distribution of the absolute value of current has also a simple form

$$P(j) = \frac{j}{\tau^2} K_0(j/\tau). \quad (27)$$

Figure 4 demonstrates excellent agreement for the numerical statistics of the current with formulae (25) and (27) for a slightly open Sinai billiard. The current distributions might be applicable even for the case of the resonant transmission through integrable billiards [56]. For this case the real eigenfunction ψ_n with the eigenenergy $\epsilon \approx \epsilon_n$ is dominant in the scattering

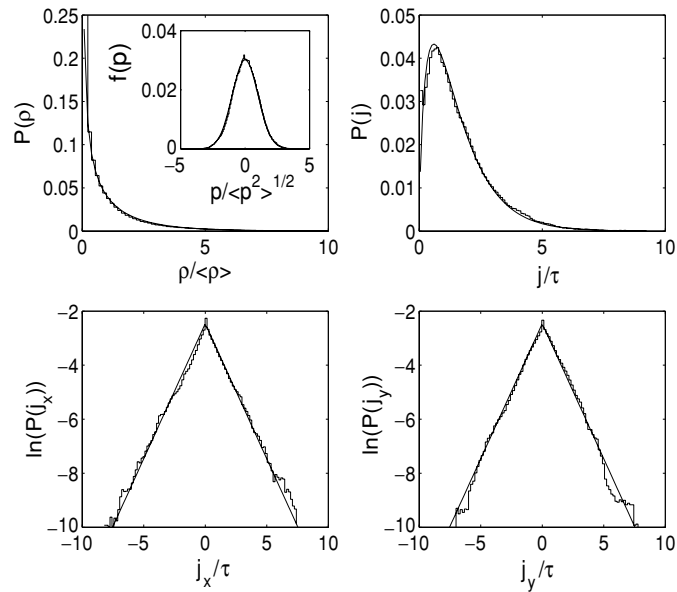


Figure 4. Statistics of current for the transmission through the Sinai billiard for $T \approx 0$. The upper left panel shows the computed distribution for $\rho = |\psi|^2$ together with the Porter–Thomas distribution $P(\rho)$ (solid curve). In the inset in the same panel the computed wavefunction statistics $f(p)$ for the real part of ψ is compared with a random Gaussian distribution (solid curve). In the right upper panel the distribution for the current density $P(j)$ is shown together with the theoretical prediction for the case $\langle j_x \rangle = 0$. Lower panels show the computed distributions for the x - and y -components of j on a logarithmic scale together with the analytic expression (25) (straight solid lines).

wavefunction (10). However since current is the imaginary part of $\psi^* \nabla \psi$, only ψ_n cannot provide the current. We are to take into account a small background of many other non-resonant eigenfunctions $\psi_n, n \neq n$ (see figure 3 for an illustration). Therefore the probability current flows only because of the background which may be considered as random noise.

There is a close similarity with planar electromagnetic cavities [1]. The basic equations take the same form and, in particular, the electric field corresponds to the quantum mechanical wavefunction and the Poynting vector is the analogue of the quantum mechanical current. It is therefore possible to experimentally observe currents, nodal points and streamlines in microwave billiards [57, 58]. In particular figure 5 [59] shows measurements for the electric field $E_z(x, y)$. Then the Poynting vector can be calculated by formula $\mathbf{j} = \frac{c}{8\pi k} \text{Im}(E_z^* \nabla E_z)$ where c is the light velocity, k is the wavenumber [57]. The microwave measurements have confirmed many of the predictions of the random Gaussian wave fields described above. For example, wavefunction statistics, current flow and various correlation functions have been verified. Note that recently scanning tunnelling spectroscopy was used to investigate the single-electron states and the corresponding squared wavefunctions [60, 61].

3. Statistics of nodal points

For a closed billiard the eigenfunctions ψ_n are the real functions. The equation $\psi_n(x, y) = 0$ determines a set of nodal lines which separate nodal domains where ψ_n is of opposite signs. Blum *et al* [62] (see also [63]) argued that the statistics of the number of these domains reflects

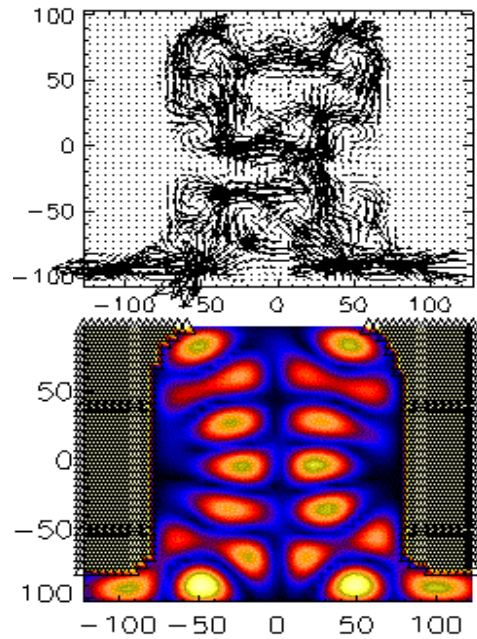


Figure 5. The measured electric field (below) and calculated Poynting vector \mathbf{j} (above) [59].

the fundamental difference between integrable and chaotic quantum systems. In [64] the distribution of nodal domains was derived analytically on the basis of a simple percolation model. In open system the wavefunction is then a scattering state with both real and imaginary parts as in (11). Then the equation $\psi_B(x, y) = 0$ gives rise to two separate sets of non-crossing nodal lines at which either u or v vanishes. The points at which the two sets of nodal lines intersect are the nodal points (NP). Since at NP $|\psi| = 0$, a phase of the ψ -function $\psi = |\psi| \exp(i\theta)$ becomes ambiguous. Explicit descriptions of NPs as phase singularities or topological charges associated with a complex wavefunction are given in many articles, for example [65–68, 70]. As Dirac demonstrated already in 1931 [65] NPs give rise to a current vortices. Moreover the vortices may be clockwise or anticlockwise, i.e. have ± 1 winding numbers. It was proven [71, 72] that neighbouring NPs on the same nodal line always have opposite winding numbers. Therefore, distribution of NPs is different from the distribution of completely random points.

Complementary to NPs there is also a different kind of peculiarity in the current flow which is related to saddles [67, 70] marked by stars in figure 6. A saddle is a nodal point in the current density $j = \sqrt{j_x^2 + j_y^2}$, i.e., the point at which the ‘current nodal lines’ $j_x = 0$ and $j_y = 0$ cross each other at nonzero u and v .

Instead of nodal lines in closed systems we are interested in the statistics of NPs for open chaotic billiards since they form vortex centres and thereby shape the entire flow pattern [73]. Thus we will focus on nodal points and their spatial distributions and try to characterize chaos in terms of such distributions. The question we wish to ask is simply if one can find a distinct difference between the distributions for nominally regular and irregular billiards. The answer to this question is clearly positive as is seen from figure 6. As shown qualitatively, NPs and saddles are both spaced less regularly in chaotic billiard in comparison to the integrable

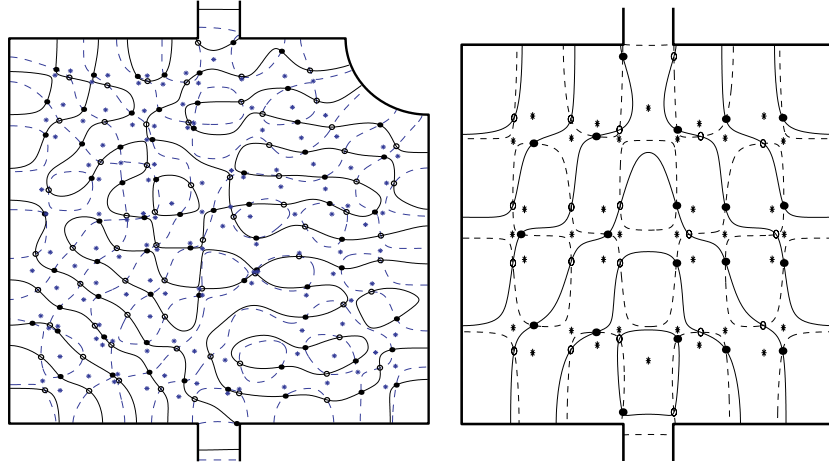


Figure 6. The complexity of nodal lines, nodal points and saddles for the transmission through chaotic (Sinai) (left) and regular billiard (right).

billiard. The mean density of NPs for a complex RGF (11) is equal to $k^2/4\pi$ [74]. This formula is satisfied with good accuracy in both chaotic and integrable billiards.

Quantitatively the disorder among points may be expressed through the correlation function of NPs and distribution of nearest distances between them. Let us introduce the density of nodal points as [75, 76]

$$d(\mathbf{r}) = |\omega(\mathbf{r}_j)|\delta(u(\mathbf{r}))\delta(v(\mathbf{r})) = \sum_j \delta(\mathbf{r} - \mathbf{r}_j), \quad (28)$$

where \mathbf{r}_j specify the NPs position, and $\omega(\mathbf{r}) = \nabla u(\mathbf{r}) \times \nabla v(\mathbf{r})$ is the vorticity. Then the correlation function of NPs can be defined as [75, 76]

$$G(s) = \left\langle \sum_{i,j} \delta(\mathbf{r} - \mathbf{r}_i)\delta(\mathbf{r} - \mathbf{r}_j - \mathbf{s}) \right\rangle. \quad (29)$$

This was considered by Halperin [77] and Liu and Mazenko [78]. Recently two teams [75, 76, 79] presented different complicated analytical expressions for the correlation function (29). Numerically however they give the same results. Experimental verification was done in microwave billiards [58]. A knowledge of the NP correlation function allows one to find the distribution function of nearest distances between NPs [76]:

$$P_{\text{NP}}(r) \approx \frac{4\pi}{\rho^{3/2}} r G(r) \left(1 - \frac{4\pi}{3\rho} \int_0^{\sqrt{\rho}r} G(s) s ds \right)^2. \quad (30)$$

It is interesting to note that distribution (30) is close to the nearest-neighbour spacing distribution of zeros of random polynomials [80]. These polynomials approximate the eigenfunctions of the unitary evolution operator of the quantum kicked rotator. It prompts us to suggest that the nearest-neighbour spacing distribution of zeros is meaningful not only for the chaotic billiards but for other quantum chaotic systems. Figure 7 shows numerical results for the transmission through the Sinai billiard [72] compared to the derived distributions. It also shows that nodal points with opposite winding numbers have a tendency to attract each other, while points with the equal winding numbers repel. Hence quantum chaos is not the

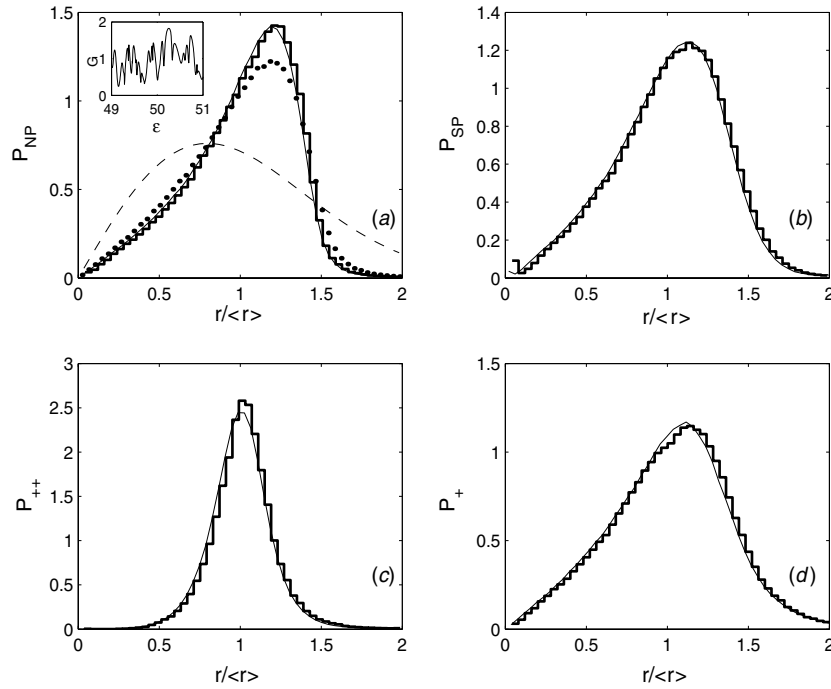


Figure 7. Distributions for separations between the nearest NPs, saddle points, NPs with the same (++) and opposite winding numbers (+−) in a chaotic Sinai billiard. The radial distribution (31) of nearest distances for completely random points is shown by the dashed curve in (a). The corresponding distribution for the Berry model function for a chaotic state (2) and random superposition of 16 eigenfunctions for a rectangular box with the same size and energy are shown by dots and thin curves, respectively.

same as complete randomness. This is also evident from the distribution for nearest neighbours among random points [81]

$$P(r) = \frac{\pi}{2} r \exp(-\pi r^2/4). \quad (31)$$

Recently Barth and Stöckmann [57] have found fair agreement of distributions shown in figure 7 with microwave experiments. Further experiments are welcome.

4. Chaotic billiards with Rashba spin–orbit interaction

Statistics of spectra and currents in the quantum systems with the spin–orbit interaction (SOI) is interesting for a number of reasons. First, even some integrable billiards such as rectangular become non-integrable in the presence of SOI [82] to give the semi-Poisson distribution for nearest level separation, while circular ones remain integrable [83]. Second, the eigenfunctions have two components as elastomechanical waves in the chaotic plates [84], which change the probability density distribution as well as the current one [85]. Moreover, the equivalence between quantum dots (QD) with SOI and the microwave billiards filled by ferrite was established [86].

Using the characteristic scale R of QD we write the Schrödinger equation in dimensionless form [82, 85]

$$-\nabla^2 \phi + \beta L \chi = \epsilon \phi \quad -\nabla^2 \chi + \beta L^+ \phi = \epsilon \chi, \quad (32)$$

where $L = \frac{\partial}{\partial x} - i \frac{\partial}{\partial y}$, $\epsilon = 2m^* R^2 E / \hbar^2$. We imply the Dirichlet boundary conditions for both components $\phi(x, y)$ and $\chi(x, y)$ in the Robnik [87] billiard. Here $\beta = 2m^* K R$, and $\hbar^2 K = 6 \times 10^{-10}$ eV cm is the SOI coefficient in a InAs structures [88]. We consider that the electric field is directed normal to the plane of QD. The confining potential is approximated by hard wall potential to consider QD as a billiard. An expression for current density can be obtained as follows [89]

$$\tilde{j} = \mathbf{j}/j_0 = -c \frac{\delta \langle H \rangle}{j_0 \delta \mathbf{A}} = \text{Im}(\Psi^+ \nabla \Psi) + \beta \Psi^+ (\mathbf{n} \times \sigma) \Psi, \quad (33)$$

where $j_0 = \frac{e\hbar}{m^* R^3}$. For small SOI constant $\beta \ll \sqrt{\epsilon}$ we can approximate the solution of (32) as [83]

$$\phi = \psi_b + O(\beta) \quad \chi = -\frac{\beta}{2} [(x + iy) - C] \psi_b = -\frac{\beta}{2} [(x - x_0) + i(y - y_0)] \psi_b, \quad (34)$$

where ψ_b are the eigenfunctions of the Schrödinger equation (1) for $\beta = 0$, $C = x_0 + iy_0$ is some arbitrary complex constant. Solution (34) demonstrates that the second component $\chi(x, y)$ increases linearly in the billiard region. Then it follows from (34) that, if the eigenfunctions ψ_b are RGF, the upper component ϕ is also RGF, whereas the lower component χ is not and depends on a shape of billiard. However, since a contribution of the component χ to the current is negligibly small, we conclude that the distributions of spin-orbit current are described by the previous formulae (25) and (27).

Similar to the free 2D electron gas the solution may be presented as $\phi = a\psi_1 + b\psi_2$ which satisfies

$$-\nabla^2 \phi_1 = \left[\epsilon + \frac{\beta^2}{2} + \frac{\beta^2}{2} \sqrt{1 + \frac{4\epsilon}{\beta^2}} \right] \phi_1, \quad (35)$$

$$-\nabla^2 \phi_2 = \left[\epsilon + \frac{\beta^2}{2} - \frac{\beta^2}{2} \sqrt{1 + \frac{4\epsilon}{\beta^2}} \right] \phi_2. \quad (36)$$

Although these equations formally look like Schrödinger equations for the billiard, in fact, they are not because the Dirichlet boundary conditions are implied only on ϕ but not separately on ϕ_1 and ϕ_2 . However for strong SOI constant $\beta \gg \sqrt{\epsilon}$ the solution consists of the ‘fast’ part with $k_1 \approx \beta$ and ‘slow’ part with $k_2 \approx \frac{\epsilon}{\beta}$. Therefore we can disregard the ‘slow’ part because of the Dirichlet boundary conditions. Then equation (35) becomes the Schrödinger equation in the chaotic billiard with real eigenfunctions as a RGF. The same takes place for the lower component χ . Because of the Kramers degeneracy, both components are a complex RGF

$$\Psi = \begin{pmatrix} \phi(\mathbf{r}) \\ \chi(\mathbf{r}) \end{pmatrix} = \begin{pmatrix} p(\mathbf{r}) + iq(\mathbf{r}) \\ t(\mathbf{r}) + iw(\mathbf{r}) \end{pmatrix}. \quad (37)$$

In order to find the distribution of, say, x component of current we need eight RGFs $\Phi = (p \ t_x \ q \ w_x \ t \ p_x \ w \ q_x)$, $p_x = \partial p / \partial x, \dots$, number of which is twice as large as compared to a ‘pure’ chaotic billiard. We refer the reader to [85] for computational details and mention here that the current distribution is a superposition of the previous universal distribution (25) with two characteristic $\tau_i = k_i \langle p^2 \rangle$. Figure 8 demonstrates very good agreement between theory and numerics.

Concluding this section we present figure 9 which shows the evolution of statistics of the upper and lower components in the Robnik billiard by increasing the SOI constant. The intermediate cases (c) and (d) $\beta \sim \sqrt{\epsilon}$ show that the statistics is not universal.

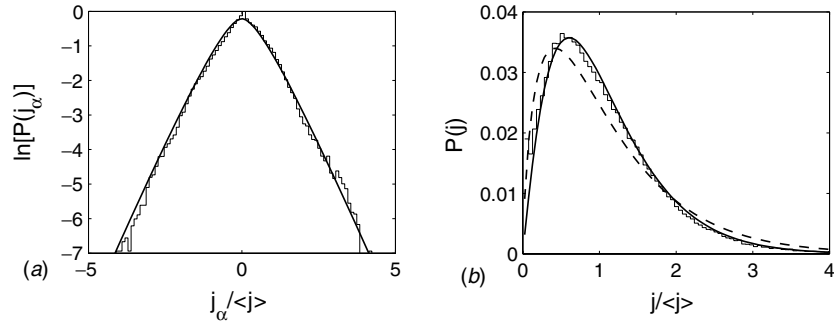


Figure 8. Current distributions $P(j_x)$ (a) and $P(j)$ (b) for the Robnik billiard for $\epsilon = 57.684$, $\beta = 50$. The dashed line shows the current distribution (27) for the ‘pure’ chaotic billiard.

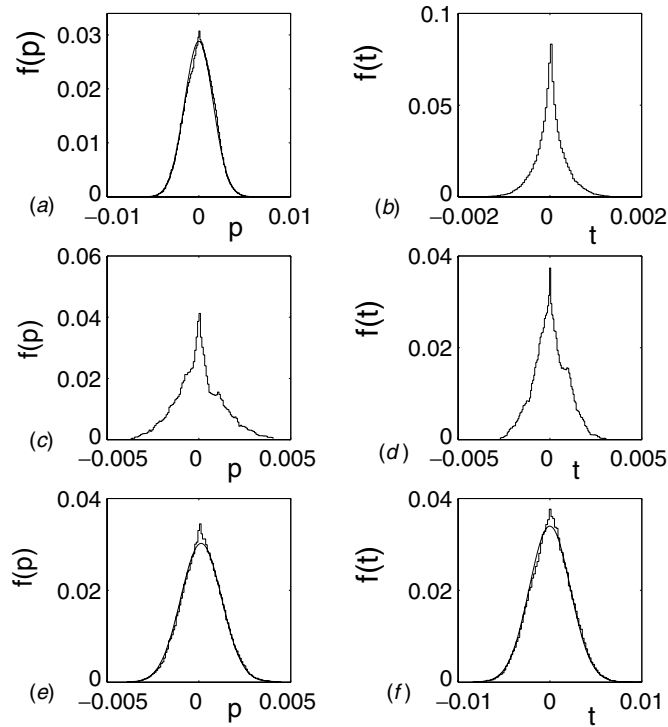


Figure 9. The numerical distributions of real parts of upper (left) and lower component (right) of the eigen spinor state for three characteristic values of β . (a, b) $\beta^2 \ll \epsilon$, ($\beta = 0.25$, $\epsilon = 522.25$), (c, d) $\beta^2 \sim \epsilon$, ($\beta = 10$, $\epsilon = 87.57$), and (e, f) $\beta^2 \gg \epsilon$, ($\beta = 50$, $\epsilon = 57.684$). Solid lines show the Gaussian distributions.

5. Electric circuit networks equivalent to chaotic quantum billiards

Electric circuit models representing a quantum particle in the one-dimensional potential were first considered by Kron in 1945 [90]. Later large random RLC networks with random mixture of capacitances and inductances [91] were intensively studied with application to

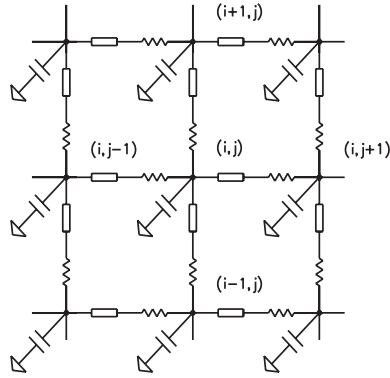


Figure 10. The first model of resonance RLC circuits.

many physical phenomena (see [92] and references therein). In particular, it was shown that fluctuations in spectra are described by usual theory of RMT [92].

There is a complete equivalence of the two-dimensional Schrödinger equation for a particle in a hard wall box to microwave billiards [1]. On the other hand, models for the equivalent RLC circuit of a resonant microwave cavity exist which establish the analogy near an eigenfrequency [93]. Therefore, there is a bridge between quantum billiards and a set of coupled RLC oscillators [94].

If to map the two-dimensional Schrödinger equation onto numerical grid $(x, y) = a_0(i, j)$, $i = 1, 2, \dots, N_x$, $j = 1, 2, \dots, N_y$ one can easily obtain an equation in the finite-element approximation

$$\psi_{i,j+1} + \psi_{i,j-1} + \psi_{i+1,j} + \psi_{i-1,j} + (a_0^2 E - 4) \psi_{i,j} = 0. \quad (38)$$

Let us consider the electric resonance circuit shown in figure 10. Each link of the two-dimensional network is given by the inductor L with the impedance $z_L = i\omega L + R$, and each site of the network is grounded via the capacitor C with the impedance $z_C = \frac{1}{i\omega C}$, where R is the resistance of the inductor and ω is the frequency. The Kirchoff's current law at each site of the network gives

$$\frac{1}{z_L} [V_{i,j+1} - V_{i,j} + V_{i,j-1} - V_{i,j} + V_{i+1,j} - V_{i,j} + V_{i-1,j} - V_{i,j}] - \frac{1}{z_C} V_{i,j} = 0, \quad (39)$$

where $V_{i,j}$ are the values of voltage at the site (i, j) . This equation coincides with the discretized version of the Schrödinger equation (38) with the eigenenergies

$$a_0^2 k^2 = -\frac{z_L}{z_C} = LC\omega^2 - iRC\omega = \frac{\omega^2}{\omega_0^2} - i\frac{\gamma\omega}{\omega_0^2}, \quad (40)$$

where $\omega_0 = 1/\sqrt{LC}$ and $\gamma = R/L$ are the eigenfrequency and the linewidth of each resonance circuit. Voltages play the role of the wavefunction of the quantum billiard. There are many ways to define the boundary conditions (BC). If the boundary sites are grounded, we obviously obtain the Dirichlet BC. If they are shunted through capacitors we obtain the free BC (the Neumann BC). Finally, if the boundary sites are shunted through resistive inductors, the BC correspond to mixed BC.

The voltage/wavefunction and current statistics in the network modelled the microwave billiard in [57] show that resonance circuits are indeed an analogue to a hard wall quantum billiard [95]. However there are three features which can make a difference when comparing

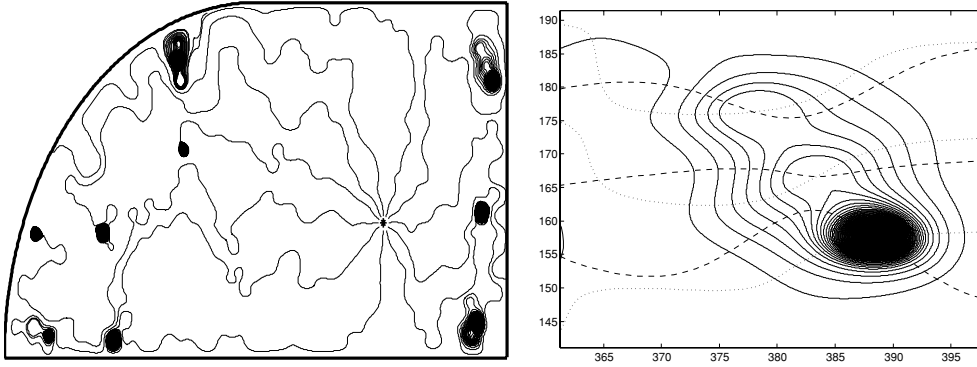


Figure 11. Left panel: quantum streamlines in a quarter of the Bunimovich billiard flowing from the point shown as a star at which the external ac voltage is applied. Right panel: zoomed part of the left figure. Solid lines show the streamlines, dashed and dotted lines are the nodal lines of the real and imaginary parts of wavefunction. The points at which the nodal lines intersecting are the centres of the vortices [72].

with quantum billiards. These are (1) a discreteness of resonance circuits, (2) tolerance of electric elements and (3) resistance of inductors. In practice the discreteness has no effect for $\lambda \geq 10a_0$ where λ is a characteristic wavelength of the wavefunction, and a_0 is the elementary unit of the network. The distribution of the wavefunction for finite grid with $a_0 = 1/100$ in fact shows extensive fluctuations compared to the Gaussian distributions because of multiple interference on discrete elements of the network [95, 96]. It is known that a noise can suppress these fluctuations. In the present case the tolerance of circuit elements, capacity and inductance play the role of noise. Therefore, the first two features of electric resonance circuits conceal each other. In fact, even a 1% tolerance substantially smoothens the distribution of the wavefunction [96].

The third feature of the electric network, resistance, has principal importance. (i) The resistance of the electric network is originated from inelastic interactions of electrons with phonons and other electrons which give rise to irreversible processes of decoherence. Therefore, the resistance acts as a reservoir which makes the quantum billiards more open. In fact, numerically computed statistics for $\rho = |V|^2$ (analogue of the probability density) shows that the statistics follow (16) with the growing parameter of openness as the resistance is increasing. (ii) The resistance R gives rise to heat losses with a local power $P = \frac{R}{2} [\text{Re}(I_x)^2 + \text{Im}(I_x)^2 + \text{Re}(I_y)^2 + \text{Im}(I_y)^2] = \frac{R}{2} [|I_x|^2 + |I_y|^2]$, where I_x, I_y are the local components of the electric current flowing between sites of the electric network. This peculiar property of large electric networks to disperse electric power was first noted by Dykhne [97]. The distribution of the heat power can be derived by the same way as was done above for the currents and has the following form [96] (see also general theory for vector statistics [98])

$$f(P) = \frac{2\mu}{v\langle P \rangle} \exp(-\mu P/\langle P \rangle) \sinh(vP/\langle P \rangle), \quad (41)$$

with μ and v given in (17).

(iii) The resistance is a simple mechanism of a deterioration of quantum coherence similar to the Büttiker one [99] and violates the equation $\nabla \mathbf{j} = 0$. In fact figure 11 demonstrates spiral behaviour of quantum streamlines [72] which sink into nodal points of the wavefunction in

system with the resistance. The characteristic localization length can easily be estimated from equation (40)

$$\lambda_R \approx \frac{4\pi a_0}{R} \sqrt{\frac{L}{C}}. \quad (42)$$

Acknowledgments

We thank the referee for many useful comments. AFS acknowledges K N Pichugin and I Rotter for many valuable discussions on the effective Hamiltonian. AFS acknowledges the Russian Foundation for Basic Research (RFBR Grant 05-02-97713 ‘Enisey’) for support. We are grateful for support from the Royal Swedish Academy of Sciences.

References

- [1] Stöckmann H-J 1999 *Quantum Chaos: An Introduction* (Cambridge: Cambridge University Press)
- [2] Wigner E P 1951 *Ann. Math.* **53** 36
Wigner E P 1955 *Ann. Math.* **62** 548
Wigner E P 1957 *Ann. Math.* **65** 203
Wigner E P 1958 *Ann. Math.* **67** 325
- [3] Porter C E and Rosenzweig N 1960 *Phys. Rev.* **120** 1698
- [4] Mehta M L and Gaudin M 1960 *Nucl. Phys.* **18** 420
Mehta M L and Gaudin M 1961 *Nucl. Phys.* **25** 447
- [5] Mehta M L 1991 *Random Matrices* (New York: Academic)
- [6] Dyson F J 1962 *J. Math. Phys.* **3** 140
Dyson F J 1962 *J. Math. Phys.* **3** 157
Dyson F J 1962 *J. Math. Phys.* **3** 166
Dyson F J 1962 *J. Math. Phys.* **3** 1191
Dyson F J 1962 *J. Math. Phys.* **3** 1199
- [7] Bohigas O, Giannoni M-J and Schmit C 1984 *Phys. Rev. Lett.* **52** 1
- [8] Efetov K B 1997 *Supersymmetry in Disorder and Chaos* (Cambridge: Cambridge University Press)
- [9] Guhr T, Müller-Groeling A and Weidenmüller H A 1998 *Phys. Rep.* **299** 190
- [10] Berggren K-F and Åberg S (ed) 2001 *Quantum Chaos Y2K: Proc. Nobel Symposium* vol 116 (Singapore: World Scientific)
Berggren K-F and Åberg S (ed) 2001 *Phys. Scr.* T **90**
- [11] Harayama T, Davis P and Ikeda K 2003 *Phys. Rev. Lett.* **90** 63901 and references within
- [12] Milner V, Hanssen J L, Campbell W C and Raizen M G 2001 *Phys. Rev. Lett.* **86** 1514
- [13] Friedman N, Kaplan A, Carasso D and Davidson N 2001 *Phys. Rev. Lett.* **86** 1518
- [14] Zhang C, Liu J, Raizen M G and Niu Q 2004 *Phys. Rev. Lett.* **93** 74101
- [15] Shapiro M and Goelman G 1984 *Phys. Rev. Lett.* **53** 1714
- [16] McDonald S W and Kaufmann A N 1988 *Phys. Rev. A* **37** 3067
- [17] Sridhar S and Heller E 1992 *Phys. Rev. A* **46** R1728
- [18] Ellegaard C, Schaadt K and Bertelsen P 2001 *Phys. Scr.* T **90** 223
- [19] Berry M V 1977 *J. Phys. A: Math. Gen.* **10** 2083
- [20] Rayleigh Lord 1945 *The Theory of Sound* (New York: Dover)
- [21] Heller E J 1984 *Phys. Rev. Lett.* **53** 1515
- [22] Tanner G 1997 *J. Phys. A: Math. Gen.* **30** 2863
- [23] Bäcker A, Schubert R and Stifter P 1997 *J. Phys. A: Math. Gen.* **30** 6783
- [24] Feshbach H H 1958 *Ann. Phys., NY* **5** 357
Feshbach H H 1962 *Ann. Phys., NY* **19** 287
- [25] Fano U 1961 *Phys. Rev.* **124** 1866
- [26] Mahaux C and Weidenmüller H A 1969 *Shell Model Approach in Nuclear reactions* (Amsterdam: North-Holland)
- [27] Sokolov V V and Zelevinsky V G 1989 *Nucl. Phys. A* **504** 562
- [28] Rotter I 1991 *Rep. Prog. Phys.* **54** 635
- [29] Albeverio S, Haake F, Kurasov P, Kuš M and Sěba P 1996 *J. Math. Phys.* **37** 4888

- [30] Fyodorov Y V and Sommers H J 1997 *J. Math. Phys.* **38** 1918
- [31] Dittes F-M 2000 *Phys. Rep.* **339** 215
- [32] Pichugin K, Schanz H and Šeba P 2002 *Phys. Rev. E* **64** 056227
- [33] Sadreev A F and Rotter I 2003 *J. Phys. A: Math. Gen.* **36** 11413
- [34] Livshits M S 1957 *Sov. Phys.—JETP* **4** 91
- [35] Verbaarschot J J M, Weidenmüller H A and Zirnbauer M R 1985 *Phys. Rep.* **129** 367
- [36] Sommers H-J, Fyodorov Y V and Titov M 1999 *J. Phys. A: Math. Gen.* **32** L77
- [37] Fyodorov Y V and Mehlige B 2002 *Phys. Rev. E* **66** 045202R
- [38] Kanzielper E and Freilikher V 1996 *Phys. Rev. B* **54** 8737
- [39] van Langen S A, Brouwer P W and Beenakker C W J 1997 *Phys. Rev. E* **55** R1
- [40] Dittes F-M, Harney H L and Müller A 1992 *Phys. Rev. A* **45** 701
- [41] Savin D V and Sokolov V V 1997 *Phys. Rev. E* **56** R4911
- [42] Savin D V, Sokolov V V and Sommers H-J 2003 *Phys. Rev. E* **67** 26215
- [43] Jalabert R A, Stone A D and Alhassid Y 1992 *Phys. Rev. Lett.* **68** 3468
- [44] Brouwer P W 2003 *Phys. Rev. E* **68** 046205
- [45] Pnini R and Shapiro B 1996 *Phys. Rev. E* **54** R1032
- [46] Šeba P, Haake F, Kuš M, Barth M, Kuhl U and Stöckmann H-J 1997 *Phys. Rev. E* **56** 2680
- [47] Ishio H, Saichev A I, Sadreev A F and Berggren K-F 2001 *Phys. Rev. E* **64** 056208
- [48] Feller W 1971 *An Introduction to Probability Theory and its Applications* (New York: Wiley)
- [49] Tribelsky M I 2002 *Phys. Rev. Lett.* **89** 070201
- [50] Saichev A I, Ishio H, Sadreev A F and Berggren K-F 2002 *J. Phys. A: Math. Gen.* **35** L87
- [51] Sadreev A F and Berggren K-F 2004 *Phys. Rev. E* **70** 26201
- [52] Lenz G and Zyczkowski K 1992 *J. Phys. A: Math. Gen.* **25** 5539
- [53] Sommers H-J and Iida S 1994 *Phys. Rev. E* **49** R2513
- [54] Kim Y-H, Kuhl U, Stöckmann H-J and Brouwer P W 2005 *Phys. Rev. Lett.* **94** 36804
- [55] Ebeling K J 1984 *Statistical Properties of Random Wave Fields in Physical Acoustics: Principles and Methods* (New York: Academic)
- [56] Sadreev A F 2004 *Phys. Rev. E* **70** 16208
- [57] Barth M and Stöckmann H J 2002 *Phys. Rev. E* **65** 066208
- [58] Kim Y-H, Barth M, Kuhl U and Stöckmann H J 2003 *Progr. Theor. Phys. Suppl.* **150** 105
- [59] Barth M 2001 *Mikrowellen-Experimente zu Leveldynamik und Wirbelbildung PhD Dissertation* Philipps-Universität, Marburg
- [60] Maltezosopoulos T *et al* 2003 *Phys. Rev. Lett.* **91** 196804
- [61] Crook R *et al* 2003 *Phys. Rev. Lett.* **91** 246803
- [62] Blum G, Gnutzmann S and Smilansky U 2002 *Phys. Rev. Lett.* **88** 114101
- [63] Foltin G, Gnutzmann S and Smilansky U 2004 *J. Phys. A: Math. Gen.* **37** 11363
- [64] Bogomolny E and Schmit C 2002 *Phys. Rev. Lett.* **88** 114102
- [65] Dirac P A M 1931 *Proc. R. Soc.* **133** 60
- [66] Nye J F and Berry M V 1974 *Proc. R. Soc. A* **336** 165
- [67] Hirschfelder J O, Christoph A C and Palke W E 1974 *J. Chem. Phys.* **61** 5435
- [68] Hirschfelder J O 1977 *J. Chem. Phys.* **67** 5477
- [69] Berry M 1981 *Singularities in waves and rays Physics of Defects* ed R Balian *et al* (Amsterdam: North-Holland)
- [70] H Wu and Sprung D W L 1993 *Phys. Lett. A* **183** 413
- [71] Freund I and Shvartsman N 1994 *Phys. Rev. A* **50** 5164
- [72] Berggren K-F, Sadreev A F and Starikov A A 2002 *Phys. Rev. E* **66** 16218
- [73] Berggren K-F, Pichigin K N, Sadreev A F and Starikov A A 1999 *JETP Lett.* **70** 403
- [74] Berry M V and Robnik M 1986 *J. Phys. A: Math. Gen.* **19** 1365
- [75] Berry M V and Dennis M R 2000 *Proc. R. Soc. A* **456** 2059
- [76] Saichev A I, Berggren K-F and Sadreev A F 2001 *Phys. Rev. E* **64** 036222
- Saichev A I, Berggren K-F and Sadreev A F 2003 *Phys. Rev. E* **65** 19903 (erratum)
- [77] Halperin B I 1981 *Statistical Mechanics of Topological Defects* ed R Balian, N Kleman and J-P Poirer (Amsterdam: North-Holland)
- [78] Liu F and Mazenko G F 1992 *Phys. Rev. B* **46** 5963
- [79] Dennis M R 2003 *J. Phys. A: Math. Gen.* **36** 6611
- [80] Leboeuf P and Shukla P 1999 *J. Phys. A: Math. Gen.* **29** 4827
- [81] Eggert J R 1984 *Phys. Rev. B* **29** 6664
- [82] Berggren K-F and Ouchterlony T 2001 *Found. Phys.* **31** 233
- [83] Bulgakov E N and Sadreev A F 2001 *JETP Lett.* **73** 505

- [84] Schaadt K, Guhr T, Ellegaard C 1 and Oxborrow M 2003 *Phys. Rev. E* **68** 36205
- [85] Bulgakov E N and Sadreev A F 2004 *Phys. Rev. E* **70** 61414
- [86] Bulgakov E N and Sadreev A F 2004 *Preprint* cond-mat/0404072
- [87] Robnik M 1983 *J. Phys. A: Math. Gen.* **16** 3971
- [88] Aronov A G and Lyanda-Geller Y B 1993 *Phys. Rev. Lett.* **70** 343
- [89] Landau L D and Lifshitz E M 1977 *Quantum Mechanics, Non-Relativistic Theory* (New York: Pergamon) chapter XVII
- [90] Kron G 1945 *Phys. Rev.* **67** 39
- [91] Clerk J P, Giraud G, Laugier J M and Luck J M 1990 *Adv. Phys.* **39** 191
- [92] Fyodorov Y V 1999 *J. Phys. A: Math. Gen.* **32** 7429
- [93] Sucher M and Fox J (ed) 1963 *Handbook of Microwave Measurements* (New York: Polytechnical Press)
- [94] Berggren K-F and Sadreev A F 2002 *Mathematical Modelling in Physics, Engineering and Cognitive Sciences: Proc. Conf. on Mathematical Modelling of Wave Phenomena* vol 7 ed B Nilsson and L Fishman (Vaxjo: Vaxjo University Press) pp 229–39
- [95] Bengtsson O, Larsson J and Berggren K-F 2005 *Phys. Rev. E* **71** 056206
- [96] Bulgakov E N, Maksimov D N and Sadreev A F 2005 *Phys. Rev. E* **71** 46205
- [97] Dykhne A M 1970 *Sov. Phys.—JETP* **59** 110
- [98] Eliyahu D 1993 *Phys. Rev. E* **47** 2881
- [99] Büttiker M 1986 *Phys. Rev. B* **33** 3020